Original Paper

Environ. Control Biol., **50** (2), 163–171, 2012

Summer-season Differences in *NDVI* and *iTVDI* among Vegetation Cover Types in Lake Mashu, Hokkaido, Japan Using Landsat TM Data

Hiroki NAITO[1], Parinaz RAHIMZADEH-BAJGIRAN[2], Yo SHIMIZU[1], Fumiki HOSOI[1] and Kenji OMASA[1]

[1] *Department of Biological and Environmental Engineering, Graduate School of Agricultural and Life Sciences, The University of Tokyo, 1–1–1 Yayoi, Bunkyo-ku, Tokyo 113–8657, Japan*

[2] *Department of Geography, University of Guelph, 50 University Avenue East, Guelph, N1G 2W1, ON, Canada*

(Received April 3, 2012; Accepted May 11, 2012)

The improved Temperature Vegetation Dryness Index (*iTVDI*) can be used as an indicator of transpiration rates in mountainous areas. We investigated the influence of vegetation cover types on differences observed in *iTVDI*, together with *NDVI* in vegetation covers around Lake Mashu in a summer day. Based on the results of comparing *NDVI* and *iTVDI* values among 14 vegetation cover types, it was shown that the vegetation cover type differences could cause significant differences in *iTVDI* values. Shrub and grassland categories showed lower *NDVI* but higher *iTVDI* values, whereas tall trees except Erman's birch showed relatively higher *NDVI* but lower *iTVDI* values. The Erman's birch *iTVDI* values were higher than the other tall trees. These results suggest that the difference of vegetation cover types could be one of the factors that influence *iTVDI* values.

Keywords : evapotranspiration, *iTVDI*, Landsat TM, *NDVI*, remote sensing

INTRODUCTION

With the increasing environmental concerns in recent years, comprehensive understanding of vegetation status in the ecosystem is required. Therefore it is needed to establish methods of monitoring plant functions at large scales. Remote sensing analysis by satellite or airborne images are useful tools to obtain comprehensive understanding of vegetation/ecosystem at regional or global scales, because remote sensing techniques enable us to measure and analyze wide vegetated areas at lower costs and times than field works especially in wide mountainous areas where field work is a difficult laborious task. In Japan, 73% of the country is classified as mountainous areas where most vegetation inhabit, therefore it is difficult to conduct regular field surveys.

The single word 'Remote sensing' covers wide categories; optical, thermal infrared, microwave, and lidar (Hobbs and Mooney, 1990; Henderson and Lewis, 1998; Omasa et al., 2007; Jones and Vaughan, 2010). In the field of vegetation remote sensing, the optical remote sensing is used for the estimation of canopy properties such as fractional vegetation cover (f_{veg}) which is defined as the fraction of surface covered by vegetation, leaf area index (*LAI*), chlorophyll content, or fraction

Corresponding author : Kenji Omasa, fax: +81–3–5841–8175,
e-mail : aomasa@mail.ecc.u-tokyo.ac.jp

of absorbed photosynthetically active radiation (*fAPAR*). On the other hand, the thermal remote sensing is used for the detection of stomatal closures and water-deficit stresses by estimating the evapotranspiration rate (Idso et al., 1981; Jackson et al., 1981; Omasa et al., 1981, 1994; Jones, 2004). Above all, T_s/VI triangle or trapezoidal method is a useful application of thermal remote sensing in heterogeneous areas which contain differing amounts of bare soil and vegetation. The method mainly estimates evapotranspiration rates by the biophysical properties encapsulated in the two dimensional feature space consisting of surface temperature (T_s) and vegetation index (*VI*) (triangle method; Price, 1990; Jiang and Islam, 1999; Sandholt et al., 2002; Nishida et al., 2003) or consisting of $T_s - T_a$ (T_a means ambient air temperature) and *VI* (trapezoidal method; Moran et al., 1994). Comprehensive reviews on the application of T_s/VI method can be found in Petropoulos et al. (2009) and Li et al. (2009).

Recently in order to apply the T_s/VI trapezoidal method to mountainous areas, Rahimzadeh-Bajgiran et al. (2012) proposed the improved Temperature Vegetation Dryness Index (*iTVDI*). The *iTVDI* is a modification of *TVDI* (Sandholt et al., 2002), which substitutes T_s axis in the TVDI feature space with $T_s - T_a$ axis for correcting the altitude effects in mountainous areas. Then, Ishimura et al. (2011) used *iTVDI* as a detecting tool of the beech forest declines in Tanzawa Mountains and concluded that *iTVDI* can detect falls in the transpiration rates by stomatal closures arising from the forest decline.

Although *iTVDI* is an indicator of transpiration rates in wide heterogeneous areas, the influence of vegetation cover types on differences observed in *iTVDI* values has not been studied yet. Vegetations are distributed in a wide range of environments and their canopy characteristics such as structures or transpiration properties depend on the dominant plant species of vegetation cover types. These canopy characteristics have the potential to influence the canopy transpiration rate and that would affect the *iTVDI* values. From the viewpoint of plant stress responses, *iTVDI* would respond to long term stresses that are plant adaptations to environmental conditions of the habitats, as well as short term stresses such as water stresses or environmental pollutions.

We also investigated Normalized Difference Vegetation Index (*NDVI*, Rouse et al., 1974), as it is a popular vegetation index and has been widely used for remote sensing of vegetation status. The principle of *NDVI* is substantially different from that of *iTVDI*; *iTVDI* estimates the transpiration rates by $T_s - T_a$, while *NDVI* estimates the amount of plant biomass such as chlorophyll content or *LAI*. Therefore the characteristics of *NDVI* would be different from that of *iTVDI* among vegetation cover types.

MATERIALS AND METHODS

The methodology of this study is shown in Fig. 1. Firstly, remote sensing data and meteorological data were pre-processed. Then *NDVI* and *iTVDI* maps were calculated. Finally the differences in both indices among 14 vegetation cover types were investigated.

Study area

The study area was chosen around Lake Mashu in the eastern part of Hokkaido prefecture shown in Fig. 3 (a). This area falls in the humid continental climate zone according to Koppen climate classification and consists of mountainous areas ranging from 123 to 1,034 meters above sea level. Therefore various plant species such as alpine shrubs, grasses, conifers or broadleaved trees inhabit in this area.

Remote sensing data

As the spatial resolution of MODIS products is not enough (MOD11: 1 km) for the analysis of each vegetation cover type (Rahimzadeh-Bajgiran et al., 2012; Ishimura et al., 2011), we selected Landsat Thematic Mapper (TM) images in order to obtain *NDVI* and T_s maps. The spatial resolutions of TM images are 30 m on the visible and near infrared bands and 120 m on the thermal

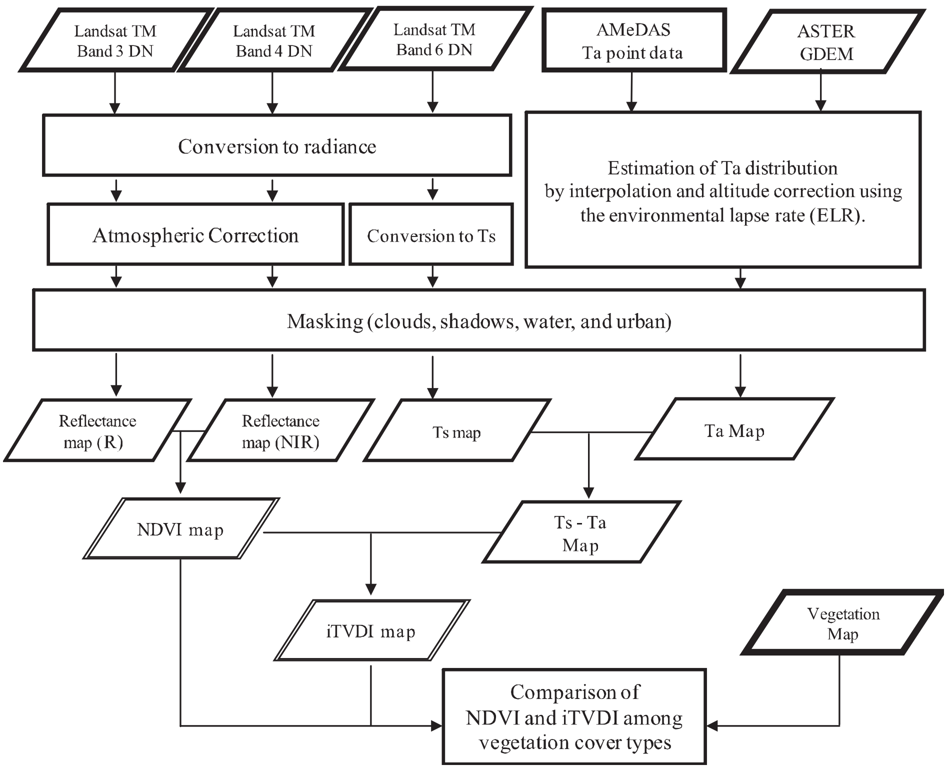

Fig. 1 Flow chart of the procedure used in this study.

band. The TM images were originally obtained from U.S. Geological Survey archives. The product level was Level 1T where a systematic radiometric correction, geometric correction and terrain correction by DEM were already done by Level 1 Product Generation System (LPGS). The acquisition date was August 6, 2006 and the scene center scan time was 10:00:59 local time. The season was summer and it was fine weather with enough water availabilities; at the Teshikaga meteorological station, near the study area, a daily precipitation was 63 mm on 4 August. Therefore it is assumed that the vegetation transpired sufficiently. Landsat red and near infrared images (band 3: 0.63–0.69 μm and band 4: 0.76–0.90 μm) and thermal image (band 6: 10.4–12.5 μm) were converted from DN to radiance by transformation (Chander and Markham, 2003). Then, the red and near infrared images were atmospherically corrected by FLAASH based on MODTRAN4 radiative transfer code within the ENVI software and converted to red and near infrared surface reflectance maps, respectively. The thermal image was converted to surface temperature (T_s) map by transformation (Chander and Markham, 2003).

Meteorological data

In order to estimate the T_a map in the study area, we used ground meteorological data acquired at AMeDAS stations (Kawayu, Teshikaga, and Kamishibetsu) supplied by Japan Meteorological Agency. At the three stations, air temperature values were measured at 10:00 A.M. on August 6, 2006. We calculated the T_a map of that time by the interpolation, estimating T_a values of each pixel by weighting the three stations temperature values using the inverse distance-weighted algorithm between each pixel and each of the three stations in the same way as Ishimura et al. (2011). Then we corrected the decrease in air temperature due to altitude by the environmental lapse rate (ELR), as defined by the International Standard Atmosphere model. Use of the ELR for altitude correction constant seems to be reasonable, because Ishimura et al. (2011) were able to have a good estimation of the air temperature distribution at Tanzawa Mountains. ASTER GDEM data provided by the Ministry of Economy, Trade and Industry of Japan (METI) and the National Aeronautics and Space Administration (NASA) was used as the elevation values of each pixel.

Masking

Using all bands of TM images, we classified each pixel in the study area into 6 categories (cloud, shadow, water, urban, soil, and vegetation) and created a mask. We masked obtained surface reflectance maps, T_s and T_a maps for excluding unnecessary pixels (cloud, shadow, water, and urban) before creating *NDVI* and *iTVDI* maps.

Calculation of NDVI and iTVDI maps

After pre-processing according to Fig. 1, we calculated *NDVI* and *iTVDI* maps. *NDVI* is defined as follows:

$$NDVI = \frac{NIR - R}{NIR + R}$$

where *NIR* is near infrared surface reflectance and *R* is red surface reflectance.

The *iTVDI* (Rahimzadeh-Bajgiran et al., 2012) is an index developed to estimate the evapotranspiration of each vegetation amount in areas with highly variable topography. The temperature difference ($T_s - T_a$) values and vegetation index (*NDVI*) values over heterogeneous area from dry bare soil to saturated bare soil and from water stressed vegetation to well watered vegetation form the trapezoidal shape scatter plots in the *iTVDI* feature space (Ishimura et al., 2011). The *iTVDI* value is defined as follows:

$$iTVDI = \frac{(T_s - T_a)_{obs} - (T_s - T_a)_{min}}{(T_s - T_a)_{max} - (T_s - T_a)_{min}}$$

where $(T_s - T_a)_{obs}$ is the observed difference between surface temperature and air temperature, and $(T_s - T_a)_{min}$ and $(T_s - T_a)_{max}$ are the minimum and maximum ($T_s - T_a$) for the same vegetation index value (e.g., *NDVI*) in the trapezoidal shape of the vegetation index vs. ($T_s - T_a$). The value of the

Table 1 Broad categories, plant groups, its legend name in vegetation map, and included pixels of vegetation cover types used in this study.

Category	Plant groups	Legend name in vegetation map	Pixels
Shrub	Siberian dwarf pine and Cowberry	*Vaccinio-Pinetum pumilae*	987
Grassland	*Sasa* spp. (Natural)	*Sasa* spp. Community	14923
	Sasa spp. (Secondary)	*Sasa* spp. Community	7856
Erman's birch	*Sasa* and Erman's birch	*Sasa* spp.-*Betula ermanii* community (Hokkaido)	21460
	Erman's birch (Secondary)	*Betula ermanii* community	39879
	Erman's birch and Jezo spruce	*Betula ermanii*, *Picea jezoensis*	38005
Conifers	Jezo spruce and Sakhalin fir	*Piceo-Abietetum sachalinensis*	8227
	Sakhalin fir (plantation)	*Abies sachalinensis* plantation	27668
	Glehn's spruce (plantation)	*Picea glehnii* plantation	47490
	Japanese larch (plantation)	*Larix kaempferi* plantation	71644
Mixed	Sakhalin fir and Water oak	*Abies sachalinensis-Quercus mongolica* ssp. *crispula* community	43096
Broadleaved	Mono maple and Water oak	*Acer mono* var. *glabrum-Quercus mongolica* ssp. *crispula* community	4467
	Silver birch and Water oak (Secondary)	*Betula platyphylla* var. *japonica-Quercus mongolica* ssp. *crispula* community	21675
	Japanese elm	*Ulmetum davidianae*	11437

iTVDI varies between 0 and 1, and it becomes higher for less evapotranspiration. By definition, to calculate the *iTVDI*, the study area should contain enough range of temperature status. In the study area some farmland soils, natural bare soils on Mt. Kamui, grasslands and shrubs showed high ($T_s - T_a$) values, while irrigated farmland soils, some croplands, and lowland tall trees showed low ($T_s - T_a$) values.

Vegetation map

We used the vegetation map provided by Biodiversity Center of Japan in order to evaluate the differences of *NDVI* and *iTVDI* among vegetation cover types. Vegetation cover types used in this study are summarized in Table 1 and their distributions are shown in Fig. 3 (a). To ensure enough number of pixels, we selected vegetation cover types that have more than almost 1,000 pixels for analysis.

Comparison of NDVI and iTVDI among vegetation cover types

We verified whether the difference in vegetation cover types caused any significant differences of *NDVI* and *iTVDI* values as follows; firstly, we calculated the averages and standard errors (SE) of *NDVI* and *iTVDI* of vegetation cover types, and then we compared both values of all vegetation cover type pairs using Tukey-Kramer HSD test.

RESULTS

NDVI and *iTVDI* maps are given in Fig. 2. *NDVI* values were generally high in vegetated regions, while *iTVDI* values appreciably varied spatially. These characteristics were in general agreement with the study at the Tanzawa Mountains (Ishimura et al., 2011).

The result of comparison is shown in Fig. 3 (b). *NDVI* values in the 14 studied vegetation cover types were high (0.88 to 0.91) and almost constant in the full range of *NDVI* in the *iTVDI* feature space (from 0.00 to 1.00), although in fact the *iTVDI* values were significantly different between vegetation cover types. The lowest *NDVI* was observed on Siberian dwarf pine and Cowberry (i), followed by Sasa spp. (Secondary) (i) and Sasa spp. (Natural) (h) in order of increasing value. These were included in the categories of shrub and grassland, and their averages were approximately 0.88. On the other hand, the highest *NDVI* was observed on Siberian fir (a), followed by Sakhalin fir and Water oak (b) and Mono maple and Water oak (b, c) in order of increasing value. Their averages were approximately 0.90 and other tall trees (Erman's birch, conifers, mixed, broadleaved) also had values around 0.90. Even though Japanese larch (g) and Japanese elm (f) had slightly lower *NDVI* values than the other tall trees, the differences (about 0.01) were just negligible amounts. To summarize the results of *NDVI* for convenience, we divided vegetation cover types into two groups; the lower group composed of shrub and grassland categories (h, i) and

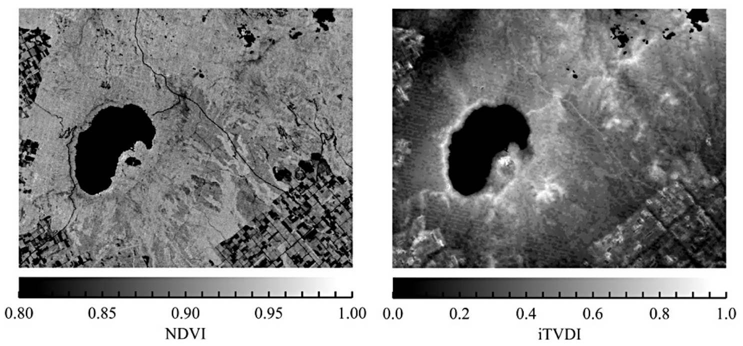

Fig. 2 The *NDVI* map and The *iTVDI* map. The black pixels mean areas where either *NDVI* (*iTVDI*) is lower than 0.80 (0.0) or there are no data because of masking.

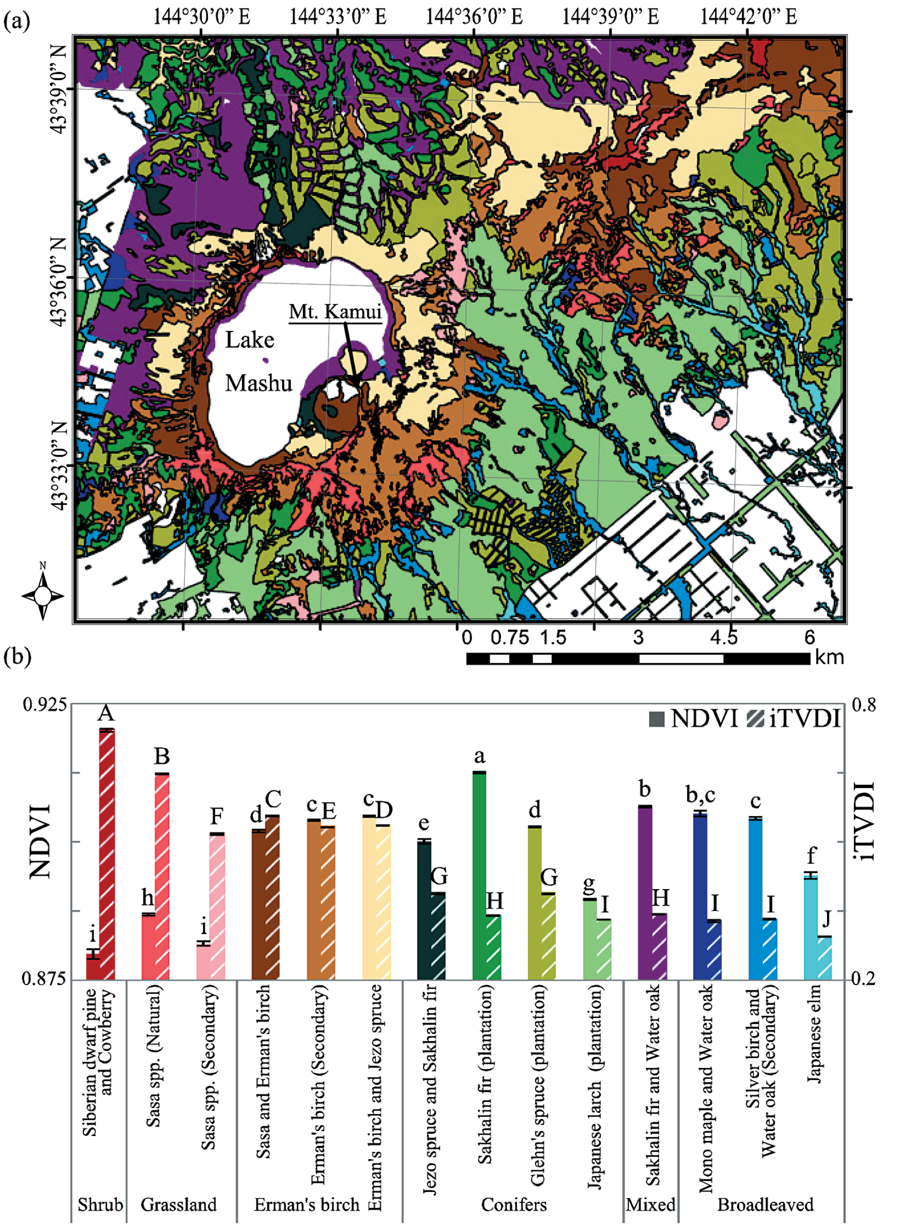

Fig. 3 (a) The study area used for the calculation of *NDVI* and *iTVDI*. Fourteen different color regions are used for comparison in this study. The colors correspond to the legend of (b). (b) Means of *NDVI* and *iTVDI* for respective vegetation cover types. The left axis shows the values of *NDVI* from 0.875 to 0.925, while the right axis shows the values of *iTVDI* from 0.2 to 0.8. Error bars represent the standard errors. Columns marked by different lowercase or uppercase letters indicate statistical significance of *NDVI* or *iTVDI* at different levels for $P < 0.05$ by Tukey-Kramer HSD test.

the higher group composed of tall trees (from a to g).

As for the *iTVDI*, the values considerably varied between vegetation cover types (from 0.29 of Japanese elm to 0.74 of Siberian dwarf pine). The lowest *iTVDI* was observed on Japanese elm (J), followed by Mono maple and Water oak (I) and Japanese larch (I) in order of increasing value.

Their averages were approximately 0.3 and tall trees except for Erman's birch (conifers, mixed, broadleaved) also indicated low values from 0.3 to 0.4. Particularly, Japanese elm showed the lowest *iTVDI* level (J) among tall trees. Although Erman's birch belongs to tall trees, it was notable that it indicated higher *iTVDI* (more than 0.53) than all other tall trees. The highest *iTVDI* was observed on Siberian dwarf pine and Cowberry (A), followed by Sasa spp. (Natural) (B) and Sasa and Erman's birch (C) in order of increasing value. Their averages were 0.74, 0.64, and 0.55, respectively. Sasa spp. (Secondary) was at the same level with Erman's birch category. According to the results of the *iTVDI*, we were able to roughly divide vegetation cover types into the following three groups; the high group (A, B) consists of shrub category and Sasa spp. (Natural), the middle group (C to F) consists of Sasa spp. (Secondary) and Erman's birch category, and the low group (G to J) consists of conifers, mixed, and broadleaved trees.

DISCUSSION

As presented above, vegetation cover types were divided into two groups based on their *NDVI* values; the lower group consists of shrub and grassland and the higher group consists of tall trees. The f_{veg} (defined as the fraction of surface covered by vegetation) and *LAI* (defined as the one sided leaf area in broadleaved trees or projected needleleaf area in conifers per unit ground area) are the factors affecting *NDVI*. *NDVI* has a positive relationship with f_{veg} or *LAI*, although the relationship between *NDVI* and *LAI* is non-linear (Jones and Vaughan, 2010). Tall trees generally have high *LAI*. By contrast, grasslands have lower *LAI*. For reference, *LAI*s of respective plant species are as follows; *LAI*s of *Sasa senanensis*, Erman's birch, Japanese larch, evergreen conifers (temperate zone), and deciduous broadleaved trees (temperate zone) are 1.85±1.17 (mean±standard deviation; Sakai and Akiyama, 2005), 4.5±1.0 (Sumida et al., 2009), 4.2 (Tsutsumi, 1989), 12, and 5 (the frequent values; Larcher, 2003), respectively. Though *LAI* of Siberian dwarf pine occasionally indicates to be over 5 (Kajimoto., 1989), it showed the lower *NDVI* value. This might have resulted from low f_{veg} due to the mixture of the shrub and rocks or soil surfaces on the top of mountains.

It is reasonable to directly compare each vegetation cover type transpiration rate by comparing *iTVDI* values (Ishimura et al., 2011). In addition, all *NDVI* values could be regarded as almost constant in the full range of *NDVI* in the *iTVDI* feature space (from 0.00 to 1.00), because the values were high (0.88 to 0.91), though there were significant *NDVI* differences in all 14 studied vegetation cover types (from a to i).

With respect to the *iTVDI*, vegetation cover types were divided into three groups; the high group consists of shrub category and Sasa spp. (Natural), the middle group consists of Sasa spp. (Secondary) and Erman's birch category, and the low group consists of conifers, mixed, and broadleaved trees. In general, high *LAI* increases the maximum transpiration rate of the canopy, and vice versa (Mauser and Schädlich, 1998). As described above, tall trees have higher *LAI* than grassland, so the lower *iTVDI* values of them are expected. As for shrubs, several factors such as low f_{veg} and transpiration properties might have caused the high *iTVDI* values.

Only Erman's birch showed relatively higher *iTVDI* values than the other tall trees. This might be explained by the reasons that the unique transpiration properties of Erman's birch would be different from the other tall trees or Erman's birch around Lake Mashu would be stressed by several reasons (Koike, 2011). However, the main cause could not be determined only from these results. Japanese elm showed the lowest *iTVDI* level in tall trees. Because it is one of the riparian trees which grow adjacent to water such as a riversides or lakesides, so the high water availability or water-body evaporation could cause the low *iTVDI*.

We could not rule out the influence of environmental stresses on *iTVDI* for Erman's birch. However, by considering at least shrubs, grasslands, and tall trees, it is conceivable that vegetation cover type differences would influence the *iTVDI* values. Thus, these results imply that the vegetation cover type differences could be one of the factors that influence *iTVDI* values. It means that the unique canopy characteristics of dominant species on vegetation cover types, such as structures (e.g. *LAI* or f_{veg}) and unique transpiration properties (e.g. the average stomatal conductance of the species), could influence the transpiration rate of canopy, which results in the significant difference in *iTVDI* values. Particularly when *iTVDI* is used as a tool for monitoring canopy stresses, we should consider the influence of stomatal closures affected by environmental stresses as well as the influence of the unique canopy characteristics of dominant species as described above.

REFERENCES

Chander, G., Markham, B. L. 2003. Revised Landsat-5 TM radiometric calibration procedures and post-calibration dynamic ranges. IEEE Transactions on Geoscience and Remote Sensing **41**: 2674–2677.

Henderson, F. M., Lewis, A. J. 1998. Principles and Application of Imaging Radar. Manual of Remote Sensing, 2. John Wiley and Sons, New York, USA, pp 896.

Hobbs, R. J., Mooney, H. A. 1990. Remote Sensing of Biosphere Functioning, Springer-Verlag, NewYork, USA, pp 312.

Idso, S. B., Jackson, R. D., Pinter, P. J., Reginato, R. J., Hatfield, J. L. 1981. Normalizing the stress-degree-day parameter for environmental variability. Agric. Meteorol. **24**: 45–55.

Ishimura, A., Shimizu, Y., Rahimzadeh-Bajgiran, P., Omasa, K. 2011. Remote sensing of Japanese beech forest decline using an improved Temperature Vegetation Dryness Index (*iTVDI*). iForest **4**: 195–199.

Jackson, R. D., Idso, S. B., Reginato, R. J., Pinter, P. J. 1981. Canopy temperature as a crop water stress indicator. Water Resour. Res. **17**: 1133–1138.

Jiang, L., Islam, S. 1999. A methodology for estimation of surface evapotranspiration over large areas using remote sensing observations. Geophysical Research Letters **26**: 2773–2776.

Jones, H. G. 2004. Application of thermal imaging and infrared sensing in plant physiology and ecophysiology. Adv. Bot. Res. incorporating Advances in Plant Pathology **41**: 107–163.

Jones, H. G., Vaughan, R. A. 2010. Remote Sensing of Vegetation. Oxford University Press, New York, USA, pp 353.

Kajimoto, T. 1989. Aboveground biomass and litterfall of *Pinus pumila* scrubs growing on the Kiso mountain range in central Japan. Ecological Research **4**: 55–69.

Koike, T., Kitao, M., Watanabe, M. 2011. "*Dakekanba no Seityo Tokusei — Tairyuken Ozon niyoru Seityo Sogai no Kanousei*" [The growth characteristics of Erman's birch — The possibility of groth inhibition due to troposheric ozone—]. Hoppo Ringyo **63**: 36–38.

Larcher, W. 2003. Physiological Plant Ecology. Springer-Verlag, Berlin, Germany, pp 450.

Li, Z. L., Tang, R., Wan, Z., Bi, Y., Zhou, C., Tang, B., Yan, G., Zhang, X. 2009. A review of current methodologies for regional evapotranspiration estimation from remotely sensed data. Sensors **9**: 3801–3853.

Mauser, W., Schädlich, S. 1998. Modeling the spatial distribution of evapotranspiration on different scales using remote sensing data. J. Hydrol. **212–213**: 250–267.

Moran, M. S., Clarke, T. R., Inoue, Y., Vidal, A. 1994. Estimating crop water deficit using the relation between surface-air temperature and spectral vegetation index. Remote Sens. Environ. **49**: 246–263.

Nishida, K., Nemani, R. R., Glassy, J. M., Running, S. W. 2003. Development of an evapotranspiration index from Aqua/MODIS for monitoring surface moisture status. IEEE Transactions on Geoscience and Remote Sensing **41**: 493–501.

Omasa, K., Hashimoto, Y., Aiga, I. 1981. A quantitative analysis of the relationships between SO_2 or NO_2 sorption and their acute effects on plant leaves using image instrumentation. Environ. Control in Biol. **19**: 59–67.

Omasa, K. 1994. Diagnosis of trees by portable thermographic system. In "Immissionsökologische Forschung im Wandel der Zeit" (ed. by Kuttler, W., Jochimsen, M.). Westarp Wissenschaften, Magdeburg, Germany, p 141–152.

Omasa, K., Hosoi, F., Konishi, A. 2007. 3D lidar imaging for detecting and understanding plant responses and canopy structure. J. Exp. Bot. **58**: 881–898.

Petropoulos, G., Carlson, T. N., Wooster, M. J., Islam, S. 2009. A review of Ts/VI remote sensing based methods for the retrieval of land surface energy fluxes and soil surface moisture. Progress in Physical Geography **33**: 224–250.

Price, J. C. 1990. Using spatial context in satellite data to infer regional scale evapotranspiration. IEEE Transactions on Geoscience and Remote Sensing **28**: 940–948.

Rahimzadeh-Bajgiran, P., Omasa, K., Shimizu, Y. 2012. Comparative evaluation of the Vegetation Dryness Index (*VDI*), the Temperature Vegetation Dryness Index (*TVDI*) and the improved TVDI (*iTVDI*) for water stress detection in semi-arid regions of Iran. ISPRS Journal of Photogrammetry and Remote Sensing **68**: 1–12.

Rouse, J. W., Haas, R. H., Schell, J. A., Deering, D. W., Harlan, J. C. 1974. Monitoring the vernal advancement and retrogradation (green wave effect) of natural vegetation. NASA/GSFC Final report, Greenbelt, MD, USA.

Sakai, T., Akiyama, T. 2005. Quantifying the spatio-temporal variability of net primary production of the understory species, *Sasa senanensis*, using multipoint measuring techniques. Agricultural and Forest Meteorology **134**: 60–69.

Sandholt, I., Rasmussen, K., Andersen, J. 2002. A simple interpretation of the surface temperature/vegetation index space for assessment of surface moisture status. Remote Sens. Environ. **79**: 213–224.

Sumida, A., Nakai, T., Yamada, M., Ono, K., Uemura, S., Hara, T. 2009. Ground-based estimation of leaf area index and vertical distribution of leaf area density in a *Betula ermanii* forest. Silva Fennica **43**: 799–816.

Tsutsumi, T. 1989. "*Shinrin Seitai Gaku*" [Forest ecology]. Asakura Publishing Co., Ltd., Tokyo, Japan, pp 166.